Sr_{2}Ir_{1−x}Rh_{x}O_{4}(x0.5): An inhomogeneous j_{eff}=1/2 Hubbard system

Shalinee Chikara, Daniel Haskel, Jae-Hoon Sim, Heung-Sik Kim, Cheng-Chien Chen, G. Fabbris, L. S. I. Veiga, N. M. Souza-Neto, J. Terzic, K. Butrouna, G. Cao, Myung Joon Han, and Michel van Veenendaal

Phys. Rev. B **92**, 081114 — Published 24 August 2015

DOI: 10.1103/PhysRevB.92.081114

$Sr_2Ir_{1-x}Rh_xO_4$ ($x < 0.5$): an inhomogeneous $j_{\rm eff} = \frac{1}{2}$ Hubbard system

Shalinee Chikara,[1] Daniel Haskel,[1] Jae-Hoon Sim,[2] Heung-Sik Kim,[2] Cheng-Chien Chen,[1] G. Fabbris,[1,3] L. S. I. Veiga,[1,4,5] N. M. Souza-Neto,[4] J. Terzic,[6] K. Butrouna,[6] G. Cao,[6,*] Myung Joon Han,[2] and Michel van Veenendaal[1,7]

[1] *Advanced Photon Source, Argonne National Laboratory, Argonne, Illinois 60439, USA*
[2] *Department of Physics, Korea Advanced Institute of Science and Technology, Daejeon 305-701, Korea*
[3] *Department of Physics, Washington University, St. Louis, Missouri 63130, USA*
[4] *Laboratório Nacional de Luz Síncrotron (LNLS), Campinas, Sao Paulo 13083-970, Brazil*
[5] *Instituto de Física Gleb Wataghin, Universidade Estadual de Campinas, Campinas, Sao Paulo 13083-859, Brazil*
[6] *Center for Advanced Materials and Department of Physics and Astronomy, University of Kentucky, Kentucky, Lexington, Kentucky 40506, USA*
[7] *Dept. of Physics, Northern Illinois University, De Kalb, Illinois 60115, USA*

(Dated: July 27, 2015)

In a combined experimental and theoretical study, we investigate the properties of $Sr_2Ir_{1-x}Rh_xO_4$. From the branching ratios of the L-edge isotropic X-ray absorption spectra, we determine that the spin-orbit coupling is remarkably independent of x for both iridium and rhodium sites. DFT+U calculations show that the doping is close to isoelectronic and introduces impurity bands of predominantly rhodium character close to the lower Hubbard band. Overlap of these two bands leads to metallic behavior. Since the low-energy states for $x < 0.5$ have predominantly $j_{\rm eff} = \frac{1}{2}$ character, we suggest that the electronic properties of this material can be described by an inhomogeneous Hubbard model, where the on-site energies change due to local variations in the spin-orbit interaction strength combined with additional changes in binding energy.

In recent years, there has been a significant interest in the electronic properties of iridium oxides. Compared to first-row transition-metal oxides, the electrons in the $5d$ orbitals experience a larger spin-orbit interaction due to the larger nuclear charge, but have a smaller electron-electron interaction as a result of the larger radial extent of the $5d$ orbitals. The low-energy physics of Ir^{4+} ($5d^5$) compounds is dominated by $j_{\rm eff} = \frac{1}{2}$ states[2–4] arising from the splitting of the t_{2g} states by the $5d$ spin-orbit interaction. Mott physics in this band causes insulating behavior for undoped compounds, such as Sr_2IrO_4. The validity of the $j_{\rm eff} = \frac{1}{2}$ states was confirmed by resonant inelastic x-ray scattering experiments[5] that showed a clear spin-wave dispersion for the pseudospins and distinct transitions between the $j_{\rm eff} = \frac{1}{2}$ and $\frac{3}{2}$ states. Considering the large widths of the t_{2g} bands, one might question the stability of the $j_{\rm eff} = \frac{1}{2}$ states. From DFT+U calculations, it is known[2] that, while the empty t_{2g} states have predominantly $j_{\rm eff} = \frac{1}{2}$ character, for the occupied states, there is an overlap of the two $j_{\rm eff}$ bands at higher binding energies. Furthermore, pressure-dependent studies[6] show that the local spin-orbit coupling is strongly reduced in Sr_2IrO_4 above 30 GPa and extrapolates to zero around 80-90 GPa. In this study, we look at $Sr_2Ir_{1-x}Rh_xO_4$ where the spin-orbit coupling is perturbed by doping with rhodium ions. Rhodium is situated directly above iridium in the periodic table and has a significantly smaller spin-orbit interaction.

The behavior of rhodium-doped iridates has puzzled researchers for several years. The doping of rhodium decreases the magnetic ordering temperature and a transition from an antiferromagnetic insulator to a paramagnetic metal is observed at $x = 0.17$[7–11]. A number of qualitative explanations have been given for the changes in the electronic structure. On the one hand, one can envision rhodium doping as an isoelectronic substitution of a $5d^5$ ion by a $4d^5$ ion[7,8]. The metal-insulator transition is then due to the tuning of the effective spin-orbit interaction in the amalgated band structure. On the other hand, it has been proposed[9–11] that the rhodium doping is not isoelectronic but inserts Rh^{3+} ($4d^6$) ions into the IrO_2 planes. To conserve charge neutrality, nearby Ir^{5+} ions are created. The effective hole doping changes the filling of the iridium bands, causing a metal-insulator transition comparable to a doped Mott-Hubbard insulator. In a combined experimental and theoretical study, we demonstrate that $Sr_2Ir_{1-x}Rh_xO_4$ is an inhomogeneous Hubbard system that conserves the $j_{\rm eff} = \frac{1}{2}$ stucture at low rhodium dopings. Although theory shows that the doping is close to isoelectronic, there is virtually no tuning of the spin-orbit interaction. The local modulation of the spin-orbit interaction between rhodium and iridium sites combined with small variations in binding energy induces states close to the top of the lower Hubbard band leading to metallic behavior for larger rhodium doping.

Figure 1 shows the isotropic X-ray absorption spectra at the L edges of polycrystalline $Sr_2Ir_{1-x}Rh_xO_4$ for several doping levels ($0 \le x \le 0.70$). Additional experimental details are given in the Supplementary Materials[12]. Of particular importance in the study of $4d$ and $5d$ materials is the intensity ratio of the L_3 and L_2 edges[6,9,14], known as the branching ratio BR $= I_{L_3}/I_{L_2}$. This quantity can be related to the spin-orbit coupling via[13] BR $= (2+r)/(1-r)$ with $r = \langle \mathbf{L}\cdot\mathbf{S}\rangle/n_h$ where n_h is the number of holes on the transition-metal site and $\langle \mathbf{L}\cdot\mathbf{S}\rangle$ is the expectation value of the spin-orbit coupling of the empty states (note that this is opposite to $\langle \mathbf{L}\cdot\mathbf{S}\rangle$ of the

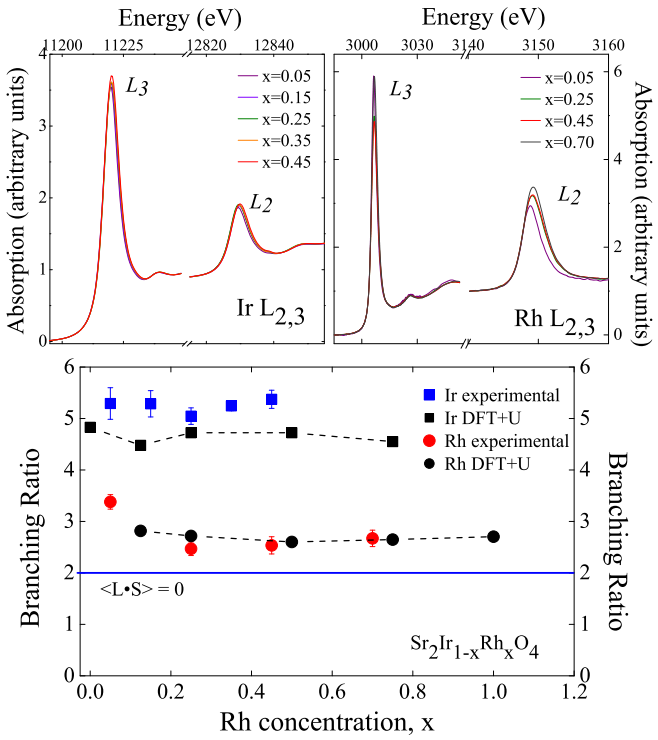

FIG. 1. The top part shows the isotropic X-ray absorption at the iridium and rhodium L edges. The bottom half gives the branching ratio (BR), *i.e.* the ratio of the integrated intensities of the L_3 and L_2 absorption edges, as a function of x. This quantity is directly related to the ground-state expectation value of the spin-orbit coupling via $\langle \mathbf{L}\cdot\mathbf{S}\rangle = n_h(\mathrm{BR}-2)/(\mathrm{BR}+1)$, where n_h is the number of holes. The Figure makes a comparison of the experimental branching ratios (with error bars) and the values obtained from DFT+U (connected by a dashed line for clarity) for $Sr_2Ir_{1-x}Rh_xO_4$.

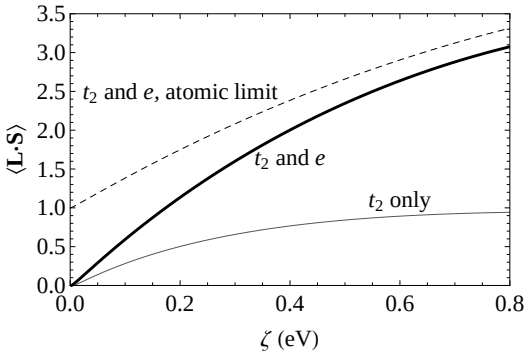

FIG. 2. Tight-binding calculation of the expectation value of the spin-orbit coupling $\langle \mathbf{L}\cdot\mathbf{S}\rangle$ (in units of $\hbar^2$) of the empty electron states as a function of the strength of the spin-orbit interaction ζ for an nd^5 transition metal compound with a finite bandwidth. The thin solid line gives the result if only t_{2g} orbitals are included; for the thick line, both t_{2g} and e_g orbitals are included. The dashed line is a comparison with an atomic calculation.

occupied states). The bottom part of Fig. 1 shows a remarkable stability of the branching ratio, apart from the Rh value for $x = 0.05$. The lack of change in the iridium branching ratio rules out the possibility of tuning of the effective spin-orbit interaction strength through rhodium doping[7,8].

Let us look at the spin-orbit coupling in more detail. There are two major contributions to $\langle \mathbf{L}\cdot\mathbf{S}\rangle$[14]. First, there is the formation of the $j_{\mathrm{eff}} = \frac{1}{2}$ moment for the t_{2g} orbitals. Even for Sr_2RhO_4, the strength of the spin-orbit interaction is sizeable ($\zeta \cong 0.15$ eV[15]), yet it has less impact on the electronic structure compared to certain $3d$ transition-metal compounds where ζ is smaller. To understand this, we need to include the effects of a finite bandwidth. Figure 2 shows the calculation of $\langle \mathbf{L}\cdot\mathbf{S}\rangle$ as a function of ζ. The simulation is done using a tight-binding model, which reproduces well the effects of a density-functional theory calculation in the absence of strong on-site interactions. When only including t_{2g} orbitals (thin line in Fig. 2), $\langle \mathbf{L}\cdot\mathbf{S}\rangle$ is close to zero for small ζ and increases steadily to the asymptotic value of 1 (in units $\hbar^2$). For iridates with $\zeta \cong 0.4$ eV, the spin-orbit coupling is relatively close to its asymptotic value. For rhodates, $\langle \mathbf{L}\cdot\mathbf{S}\rangle$ is strongly reduced by band effects. For small ζ, there is a strong difference with a calculation for a single ion (dashed line in Fig. 2), where $\langle \mathbf{L}\cdot\mathbf{S}\rangle$ jumps discontinuously from 0 to 1 when a finite spin-orbit interaction is introduced. This clearly shows that band effects are responsible for the reduction in the spin-orbit coupling[6,14]. An understanding of the reduction can be obtained by considering a simple model with a single hole per site in shifted square $j_{\mathrm{eff}} = \frac{3}{2}, \frac{1}{2}$-bands. The j_{eff} states arise from the t_{2g} orbitals and have $\langle \mathbf{L}\cdot\mathbf{S}\rangle = -0.5, 1$, respectively. If both bands have the same band width W, a relative displacement of $\frac{3}{2}\zeta$ induces a spin-orbit coupling $\langle \mathbf{L}\cdot\mathbf{S}\rangle = 3\zeta/W$, reaching the maximum value of 1 for $\zeta = W/3 \cong 0.5$ eV for a typical band width of $W = 1.5$ eV. For rhodates and iridates, this gives $\langle \mathbf{L}\cdot\mathbf{S}\rangle = 0.3$ and 0.8 with $\zeta = 0.15$ and 0.4 eV, respectively, close to the values obtained with a more elaborate calculation, see thin line in Fig. 2. A strongly reduced $\langle \mathbf{L}\cdot\mathbf{S}\rangle$ value is not in contradiction with the observation of strong spin-orbit coupling effects at the Fermi surface[16]. Whereas the former is indicative of the absence of a strong local $j_{\mathrm{eff}} = \frac{1}{2}$, the latter only affects a very limited number of electrons close to the chemical potential.

The second contribution to $\langle \mathbf{L}\cdot\mathbf{S}\rangle$ comes from the coupling of the $j_{\mathrm{eff}} = \frac{3}{2}$ with the e_g orbitals. For $\zeta \ll 10Dq$, where $10Dq \cong 3$ eV is the cubic crystal field, this adds $12\zeta/(10Dq) \cong 1.6$ to $\langle \mathbf{L}\cdot\mathbf{S}\rangle$[14], see the solid line in Fig. 2. Note that the spin-orbit coupling continues to increase for larger spin-orbit interaction strength ζ. Only in the limit that the spin-orbit interaction dominates ($\zeta \gg W, 10Dq$) does $\langle \mathbf{L}\cdot\mathbf{S}\rangle$ approach the asymptotic limit of 5 corresponding to five holes in the $j = \frac{5}{2}$ states, where the $j = \frac{5}{2}, \frac{3}{2}$ states branch from all the d orbitals.

In order to understand the effects of rhodium substitution in an iridate, we performed density functional theory (DFT+U) calculations. The spin-orbit interaction was treated within a fully relativistic j-dependent pseudopotential scheme. For additional details, see the Supplementary Materials[12]. Figure 3 shows the results for $Sr_2Ir_{1-x}Rh_xO_4$ with $x = 0, 0.125, 0.25$ and 1. Since we include all d orbitals in the calculation of the spin-orbit coupling, we project onto the $j = \frac{5}{2}, \frac{3}{2}$ states. The $j_{\text{eff}} = \frac{1}{2}$ states branch directly from $j = \frac{5}{2}$; the $j_{\text{eff}} = \frac{3}{2}$ states are a mixture of both j values. In the limit $10Dq \gg \zeta$, the ratio of $j = \frac{5}{2}, \frac{3}{2}$ character in the $j_{\text{eff}} = \frac{3}{2}$ band is 40:60, giving $\langle \mathbf{L} \cdot \mathbf{S} \rangle = 0$. For iridates, this has dropped to 30:70.

Sr_2IrO_4 shows the well-known formation of a Hubbard-like model where the lowest electron-removal and addition states have predominantly $j_{\text{eff}} = \frac{1}{2}$ ($j = \frac{5}{2}$) character, see Fig. 3(a). However, states further away from the top of the valence band have a mixed $j = \frac{5}{2}, \frac{3}{2}$ character, indicative of $j_{\text{eff}} = \frac{3}{2}$. We obtain a band gap of 0.45 eV. The calculated spin-orbit coupling is $\langle \mathbf{L} \cdot \mathbf{S} \rangle = 2.4$. Sr_2RhO_4 is, as expected, a metal with a mixed $j = \frac{5}{2}, \frac{3}{2}$ character at the Fermi level indicative of the reduced spin-orbit coupling. The expectation value $\langle \mathbf{L} \cdot \mathbf{S} \rangle = 0.95$ is reduced 60% compared to Sr_2IrO_4, see Fig. 3(d). The branching ratios obtained from these expectation values compare well with the experimental ones, see Fig. 1.

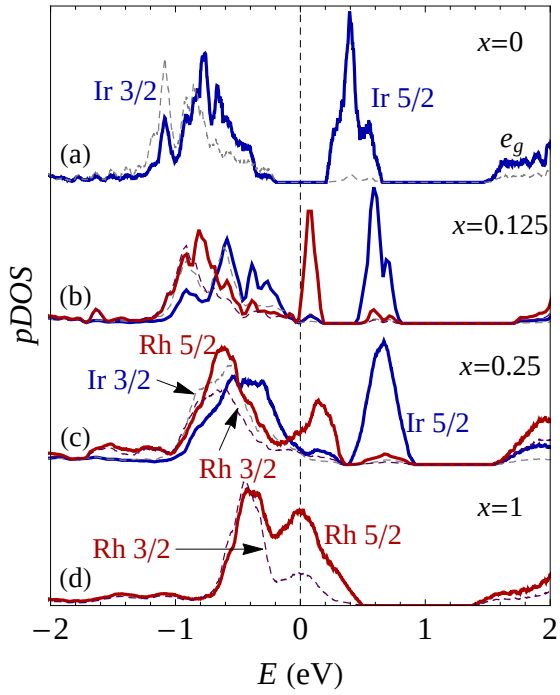

FIG. 3. DFT+U calculation of the density of states for $Sr_2Ir_{1-x}Rh_xO_4$ with $x = 0, 0.125, 0.25$, and 1 shown in (a)-(d), respectively. The projected $j = \frac{5}{2}, \frac{3}{2}$ (solid and dashed, respectively) densities of states for iridium (blue/gray) and rhodium (red/purple) are shown. For a better comparison, the projected densities of states of iridium and rhodium are normalized to their integrated intensity.

Fig. 3(b) shows the calculation for $x = 0.125$. We see that a narrow impurity-like band of predominantly rhodium character appears inside the gap close to the lower Hubbard band. The Fermi level lies inside a 39 meV gap. Figure 3(c) shows the results for $Sr_2Ir_{0.75}Rh_{0.25}O_4$. We see that the rhodium states broaden and now overlap with the iridium bands, causing metallic behavior. There are a number of salient differences with earlier suggested changes in the electronic structure[7–11]. The broad features of the iridium projected density of states remain largely intact. Therefore, there is little indication of spin-orbit tuning with the energy difference between the $j = \frac{5}{2}$ and $\frac{3}{2}$ almost unchanged. In addition, there is only a small reduction of 30 meV in the energy between the upper and lower Hubbard bands in the iridium projected densities of states. The presence of states inside the Hubbard gap has also been observed with optical spectroscopy[7] and was interpreted as the emergence of quasiparticle states comparable to that observed in dynamical mean-field theory[17]. However, since these states are already present in a DFT+U calculation, this assignment is unlikely. Alternatively, these empty states could be related to hole doping into the lower Hubbard band[9,10]. However, a calculation of the change in electron densities shows that the variations are 0.16 electrons or less compared to the undoped compounds. The rhodium substitution is therefore very close to isoelectronic. This appears to contradict the results in Refs.[9–11] based on the chemical shifts of the Rh L-edge X-ray absorption spectra.

Analysis of the results shows that the density of states close to the Fermi level can be approximated by an inhomogenous $j_{\text{eff}} = \frac{1}{2}$ Hubbard model. Although the doping is close to isoelectronic, there are significant local modulations of the strength of the spin-orbit interaction plus additional small chemical shifts. The reduction in ζ of 0.25-0.3 eV for the rhodium sites is sufficient to pull states from the upper Hubbard band into the 0.45 eV gap. These states subsequently merge with the lower Hubbard band to cause metallic behavior. Surprisingly, the states close to the Fermi level retain their $j_{\text{eff}} = \frac{1}{2}$ ($j = \frac{5}{2}$) character. Where the states at the Fermi level in Sr_2RhO_4 have a mixed $j = \frac{5}{2}, \frac{3}{2}$ character, the $j = \frac{3}{2}$ weight in the rhodium partial density of states is suppressed in the mid gap states. This is due to the enhanced mixing between the mid-gap $j = \frac{5}{2}$ states and similar states in the lower Hubbard band. This also leads to the presence of iridium density of states in the mid-gap states.

The DFT+U calculations show that the low-energy electronic structure of $Sr_2Ir_{1-x}Rh_xO_4$ has predominantly $j_{\text{eff}} = \frac{1}{2}$ character. Rhodium doping leads to the appearance of impurity-like bands close to the lower Hubbard band. We therefore propose that the low-energy properties can, to lowest order, be described by a inhomogeneous Hubbard model

$$H = \sum_{i\sigma} \varepsilon_i c^\dagger_{i\sigma} c_{i\sigma} - t \sum_{\langle ij \rangle \sigma} (c^\dagger_{j\sigma} c_{i\sigma} + \text{H.c}) + U \sum_i n_{i\uparrow} n_{i\downarrow},$$

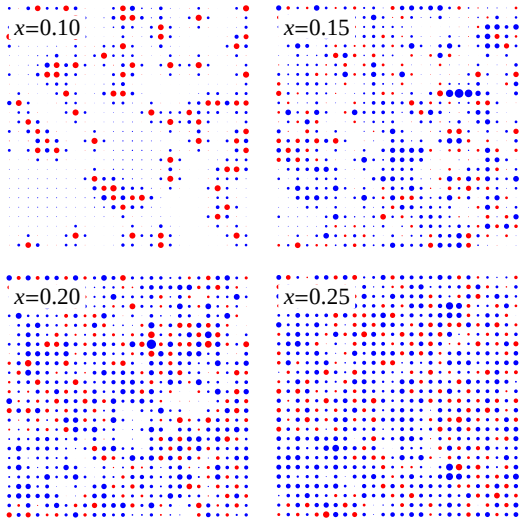

FIG. 4. Local variations in electron density on the transition-metal sites in $Sr_2Ir_{1-x}Rh_xO_4$ for $x = 0.10, 0.15, 0.20$, and 0.25 using an inhomogeneous Hubbard model in the Hubbard-I approximation. The area of the circles corresponds to the change in electron density, where red/blue indicates an increase/decrease of the electron density with respect to 1. All the rhodium sites have an increased density (red). The variations in electron density are less than 0.1.

where $\sigma = \uparrow, \downarrow$ represents the two degrees of freedom in the $j_{\rm eff} = \frac{1}{2}$ states. The last two terms on the right-hand side are the usual Hubbard model with an on-site repulsion U and where $\langle ij \rangle$ indicates nearest-neighbor hopping. The first term indicates the inhomogeneities introduced by the local variations in the spin-orbit interaction strength ζ in combination with additional changes in the binding energy. This system differs somewhat from the usual inhomogenous models[20] in that there is almost no variation in the on-site energies of the doped sites. We use this model to further investigate the electronic structure of $Sr_2Ir_{1-x}Rh_xO_4$. To calculate larger systems we apply the Hubbard-I approximation[18], where the local Green's function is given by

$$G^0_{i\sigma} = \frac{1 - n_{i,\sigma}}{\hbar\omega - \varepsilon_i + \mu + i0^+} + \frac{n_{i,\sigma}}{\hbar\omega - \varepsilon_i + \mu + U + i0^+} \quad (1)$$

which is used in obtaining the full Green's function that includes the hopping between different sites[12]. To obtain an effective single-particle model, the operators $n_{i,\sigma}$ are replaced by numbers and solved self-consistently. The spectral function (shown in the Supplementary Materials[12]) shows the same features as the DFT+U calculations, *i.e.* two Hubbard bands and mid-gap states close to the lower Hubbard band, for $t = 0.14$ eV, $U = 0.5$ eV, and $\varepsilon_i = -0.3, 0$ eV for rhodium and iridium sites, respectively. The difference in on-site energies is comparable to the variation in the spin-orbit interaction strength. In addition, exact diagonalization results on 16 site systems show similar results. The changes in electron density are less than 0.1, in agreement with DFT, showing that there are only minor variations in the electron density. Figure 4 shows the variations in electron densities. For low doping ($x = 0.10$ and 0.15), we see that the density on the iridium sites is decreased close to the rhodium sites to compensate for the increased density on rhodium. For $x = 0.10$, the density on iridium sites more than a couple of lattice spacings removed from a rhodium is barely affected. For $x = 0.15$, we see in addition to the hole density close to the rhodium ions, an increase in the areas further removed from the rhodium ions. The density shows a Friedel-type behavior. For $x = 0.20$ and 0.25, the hole density on the iridium sites becomes more homogeneous.

In conclusion, using X-ray absorption sum rules, we have demonstrated that the spin-orbit coupling on both iridium and rhodium sites has a small x dependence in the compound $Sr_2Ir_{1-x}Rh_xO_4$. This rules out the mechanism of spin-orbit tuning[7,8], where the smaller spin-orbit interaction strength of rhodium reduces the total spin-orbit coupling leading to a metal-insulator transition. The DFT+U calculations show that the rhodium doping is close to isoelectronic. The doping leads to the appearance of impurity-like bands inside the Mott gap. For larger x, these bands broaden and overlap with the lower Hubbard band leading to metallic behavior. Since the rhodium states are inside the gap, the changes in electron densities are small. An issue that requires further theoretical investigation is the long-range magnetic order, which is known to disappear at $x = 0.17$[7–11]. Exact diagonalization results on a 16 site inhomogeneous Hubbard model show that impurity-type doping is much less effective at reducing the magnetization than hole doping, showing a 10% and 40% decrease in on-site magnetization, respectively, from $x = 0$ to 0.5. Although the on-site magnetization is still finite, the long-range order appears to extrapolate to zero after rhodium doping. Finally, Figure 1 seems to indicate that for very low rhodium dopings, the spin-orbit coupling on the rhodium site is actually larger than that observed in Sr_2RhO_4. This implies that the iridium surroundings enhance the spin-orbit coupling on the rhodium site. This effect is not well reproduced by the DFT+U calculations and requires further investigation.

Acknowledgments.– Work at Argonne National Laboratory was supported by the U. S. DOE, Office of Science, Office of Basic Energy Sciences, under contract No. DE-AC02-06CH11357. M.v.V. was supported by the U. S. Department of Energy (DOE), Office of Basic Energy Sciences, Division of Materials Sciences and Engineering under Award No. DE-FG02-03ER46097 and NIU's Institute for Nanoscience, Engineering, and Technology. The computational work was partially performed at NERSC, which is supported by the U.S. DOE Contract No. DE-AC02-05CH11231. Computational resources were partly supported by the National Institute of Supercomputing and Networking/Korea Institute of Science and Technology Information with supercomputing resources including technical support (Grant No. KSC-2013-C2-23). J.

H.S. and M.J.H were supported by Basic Science Research Program through NRF (2014R1A1A2057202) and by Samsung Advanced Institute of Technology (SAIT). H.-S. K. was supported by Basic Science Research Program through the National Research Foundation of Korea (NRF) funded by the Ministry of Education (Grant No. 2013R1A6A3A01064947). The work at the University of Kentucky was supported by NSF via Grant No.DMR-1265162.

* Currently at Department of Chemistry, University of Kentucky, Lexington, KY 40506, USA.

[2] B. J. Kim, H. Jin, S. J. Moon, J.-Y. Kim, B.-G. Park, C. S. Leem, J. Yu, T. W. Noh, C. Kim, S.-J. Oh, J.-H. Park, V. Durairaj, G. Cao, and E. Rotenberg, Phys. Rev. Lett. 101, 076402 (2008).

[3] B. J. Kim, H. Ohsumi, T. Komesu, S. Sakai, T. Morita, H. Takagi, and T. Arima, Science 323, 1329 (2009).

[4] G. Jackeli and G. Khaliullin, Phys. Rev. Lett. 102, 017205 (2009)

[5] J. Kim, D. Casa, M. H. Upton, T. Gog, Young-June Kim, J. F. Mitchell, M. van Veenendaal, M. Daghofer, J. van den Brink, G. Khaliullin, and B. J. Kim Phys. Rev. Lett. **108**, 177003 (2012).

[6] D. Haskel, G. Fabbris, Mikhail Zhernenkov, P. P. Kong, C. Q. Jin, G. Cao, and M. van Veenendaal Phys. Rev. Lett. **109**, 027204 (2012).

[7] J. S. Lee, Y. Krockenberger, K. S. Takahashi, M. Kawasaki, and Y. Tokura, Phys. Rev. B 85, 035101 (2012).

[8] T. F. Qi, O. B. Korneta, L. Li, K. Butrouna, V. S. Cao, X. Wan, P. Schlottmann, R. K. Kaul, and G. Cao, Phys. Rev. B 86, 125105 (2012).

[9] J. P. Clancy, A. Lupascu, H. Gretarsson, Z. Islam, Y. F. Hu, D. Casa, C. S. Nelson, S. C. LaMarra, G. Cao, and Young-June Kim, Phys. Rev. B **89**, 054409 (2014).

[10] Y. Klein and I. Terasaki, J. Phys.: Condens. Matter 20, 295201 (2008); Y. Klein and I. Terasaki, J. Electron. Mater. 38, 1331 (2009).

[11] Y. Cao, Bull. Am. Phys. Soc. 58, C1.00004 (2013), http://meetings.aps.org/link/BAPS.2013.MAR.C1.4.

[12] see Supplementary Materials at [URL will be inserted by publisher].

[13] G. van der Laan and B.T. Thole, Phys. Rev. Lett. **60**, 1977 (1988).

[14] M. A. Laguna-Marco, D. Haskel, N. Souza-Neto, J. C. Lang, V. V. Krishnamurthy, S. Chikara, G. Cao, and M. van Veenendaal Phys. Rev. Lett. **105**, 216407 (2010).

[15] C. Martins, M. Aichhorn, L. Vaugier, and S. Biermann, Phys. Rev. Lett. 107, 266404 (2011).

[16] M. W. Haverkort, I. S. Elfimov, L. H. Tjeng, G. A. Sawatzky, and A. Damascelli Phys. Rev. Lett. **101**, 026406 (2008).

[17] M. J. Rozenberg, G. Kotliar, H. Kajueter, G. A. Thomas, D. H. Rapkine, J. M. Honig, and P. Metcalf, Phys. Rev. Lett. **75**, 105 (1995).

[18] J. Hubbard, Proc. Roy. Soc. (London) A **281**, 401 (1964).

[19] S. Chikara *et al.*, to be published.

[20] see, for example, P.J.H Denteneer, M Ulmke, R.T Scalettar, and G.T Zimanyi, Physica A **251**, 162 (1998); D. Heidarian and N. Trivedi, Phys. Rev. Lett. **93**, 126401 (2004).